JOURNAL OF AGRICULTURAL AND FOOD CHEMISTRY

ARTICLES

NMR Signal Analysis To Attribute the Components to the Solid/Liquid Phases Present in Mixes and Ice Creams

FRANÇOIS MARIETTE* AND TIPHAINE LUCAS

Cemagref, Process Engineering Technology Research Unit, 17 avenue de Cucillé, F-35044 Rennes Cedex, France

The NMR relaxation signals from complex products such as ice cream are hard to interpret because of the multiexponential behavior of the relaxation signal and the difficulty of attributing the NMR relaxation components to specific molecule fractions. An attribution of the NMR relaxation parameters is proposed, however, based on an approach that combines quantitative analysis of the spin−spin and spin−lattice relaxation times and the signal intensities with characterization of the ice cream components. We have been able to show that NMR can be used to describe the crystallized and liquid phases separately. The first component of the spin−spin and spin−lattice relaxation describes the behavior of the protons of the crystallized fat in the mix. The amount of fat crystals can then be estimated. In the case of ice cream, only the spin−lattice relaxation signal from the crystallized fraction is relevant. However, it enables the ice protons and the protons of the crystallized fat to be distinguished. The spin−lattice relaxation time can be used to describe the mobility of the protons in the different crystallized phases and also to quantify the amount of ice crystals and fat crystals in the ice cream. The NMR relaxation of the liquid phase of the mix has a biexponential behavior. A first component is attributable to the liquid fraction of the fat and to the sugars, while a second component is attributable to the aqueous phase. Overall, the study shows that despite the complexity of the NMR signal from ice cream, a number of relevant parameters can be extracted to study the influence of the formulation and of the process stages on the ice fraction, the crystallized fat fraction, and the liquid aqueous fraction.

KEYWORDS: Ice; fat crystal; multiexponential; spin−lattice relaxation; spin−spin relaxation; emulsion; foam; NMR

INTRODUCTION

Because of the structural and chemical complexity of ice cream, its characterization requires a wide range of physical techniques such as differential scanning calorimetry (DSC), nuclear magnetic resonance (NMR), electron spin resonance (ESR), and/or microscopy (*1*).

The ice crystal size can be obtained from the quantitative analysis of classical light microscopy images (*2*). The microstructure of ice cream, i.e., air bubbles, fat globules, and ice crystals, can be examined in the hydrated state by low temperature scanning electron microscopy (*3*, *4*). These microscopic techniques are very effective in providing structural information on the effect of processing conditions and of added stabilizer or surfactant, but they nevertheless fail to provide quantitative information such as the amount of ice or fat crystals.

The amount of ice is commonly measured by differential thermal analysis or DSC. The total amount of ice can be calculated from the enthalpy of fusion of water and the amount of unfrozen water from the total amount of water present in the product. In the case of ice cream, the contribution of fat enthalpy to the thermal changes is neglected when calculating the total frozen water fraction (*5*, *6*).

NMR can be used to determine the amount of unfreezable water (*7*−*10*). The amount of ice and liquid water phases can also be determined as the NMR relaxation time parameter of the liquid water protons is easily separated from that of the ice protons. Moreover, the NMR relaxation time of liquid water is sensitive to the macromolecule structure as a result of water−macromolecule interactions, so structural modifications can be detected (*11*). This technique has not to our knowledge been applied to ice cream to measure either the ice content or the mobility of the freeze-concentrated phase.

The separate behavior of the freeze-concentrated phase is the most difficult to study. It has been simulated in a number of

* To whom correspondence should be addressed. Tel: 33(0)2.23.48.21.21. Fax: 33(0)2.23.48.21.15. E-mail: francois.mariette@cemagref.fr.

10.1021/jf049294o CCC: $30.25
Published on Web 02/09/2005

studies, usually based on a series of solutions containing the main food solutes plus decreasing amounts of water. Sugar-containing solutions are usually studied as they mimic the freezing behavior of most foodstuffs, and the same approach can also be applied to mixes (*12*). Conventional measurements can be performed on the samples either at ambient temperature or at subfreezing temperatures, provided in the latter case that the samples remain unfrozen. In the first case only, the concentration effect is taken into account, whereas temperature and concentration effects are combined in the second. Possible measurements include rheological measurements (*12*), NMR diffusion and relaxation measurements (*13*), and translational and rotational molecular mobility using ESR (*14*). The glass transition temperature T_g' serve to identify the transition of the freeze concentrated phase to the amorphous state. The mobility is dramatically reduced. The remaining water is unfreezable, and chemical and enzymatic reactions are stopped or greatly slowed. Glass transitions are usually determined by DSC, thermomechanical analysis, dielectric spectroscopy, or NMR.

The international standard (ISO) method for the quantification of the amount of fat crystals is NMR (*15*). However, the reference method applies only to anhydrous fat. A number of solutions have been proposed to take the water NMR signal into account in emulsion systems where the water phase remains liquid, e.g., ref *16*. Generally, the interpretation of the NMR signal in more complex fat-containing food systems is complicated by the difficulty of attributing the different relaxation times to the different proton components: water, fats, proteins, and carbohydrates (*17*, *18*).

The DSC technique is also used with emulsions. However, the total amount of milk fat crystals cannot be quantified as the fat has to reach very low temperatures, at which the water also crystallizes. In this temperature range, the thermal changes due to the melting of the fat are negligible as compared to those due to the melting of the ice.

Generally, in the case of frozen systems such as ice cream, which include fat−water emulsions, the coexistence of crystallized and liquid fat and of crystallized and liquid water considerably complicates the interpretation of the measurement. The experimental strategies used to overcome this difficulty usually require the ice crystals to be "suppressed". This allows the characteristics of the fat globules or of the freeze-concentrated phase to be obtained. For instance, the distribution in diameter of the fat globule particles in ice cream is conventionally studied using thawed samples dissolved in a solvent, e.g., ref *19*. The fraction of solid fat as a function of temperature has been tentatively assessed by NMR by lowering the temperature of mix samples to which sodium chloride had been added to lower the freezing point of the water (*20*). It should be emphasized that such strategies often induce a bias (by either partially modifying the structure of the system or not reproducing the real system), and this can raise doubts about the conclusions.

The aim of the present work is to develop a nondestructive NMR method to characterize the behavior of both fat and water in ice cream in the frozen state. As previously mentioned, the main difficulty is to interpret the NMR signal so that the behavior of each phase (solid fat, liquid fat, liquid water, and solid water) can be distinguished.

MATERIALS AND METHODS

Sample Composition. Four formulations containing two types of fat, milk fat (F1) or refined copra fat (F2), and two types of emulsifiers were used (**Tables 1** and **2**). The emulsifiers were saturated monodiglycerides (Lygomme FM 3000 Series, Degussa Texturant Systems) and partially unsaturated monodiglycerides (Lygomme FM 4000 Series, Degussa Texturant Systems). The four formulations, labeled P2F1E2/1, P2F2E1/1, P2F1E1/1, P2F2E2/1, are part of a wider experimental design that varies the type of proteins, material, and emulsifier (eight formulations). The results of the full study will be presented in other papers (*21*, *22*). A study of the raw materials was carried out in parallel. They consisted of the two types of fat (F1 and F2) and the aqueous phase. The aqueous phases were prepared under the same conditions as the mixes. Unlike the mixes, the aqueous phases contained no emulsifier (**Table 2**).

Table 1. Two-Factor Experimental Design with Two Levels of Each Factor[a]

identification code	fat type	emulsifier type
P2F1E2/1	F1	E2
P2F2E1/1	F2	E1
P2F1E1/1	F1	E1
P2F2E2/1	F2	E2

[a] F1, milk fat; F2, refined copra fat; E1, saturated monodiglycerides (Lygomme FM 3000 Series, Degussa Texturant Systems); E2, partially unsaturated monodiglycerides (Lygomme FM 4000 Series, Degussa Texturant Systems).

Table 2. Composition of Mixes

	mix	aqueous phase (before incorporation of fat and emulsifier)
fat	8.00	
water	65.22	70.89
glucose syrup	4.69	5.10
sucrose	12.28	13.35
lactose	6.57	7.14
protein	2.11	2.29
stabilizer	0.13	0.14
ash	1.00	1.09

Sample Preparation. All samples were prepared by Degussa Texturant Systems (Baupte, France). The mixes were prepared in the morning, matured in the afternoon, stored overnight at 4 °C, and then frozen the following day (ice cream).

Mixing. Water was added to the blend of powders. Meanwhile, fat and glucose syrup were heated at 45 °C and then mixed together and further heated at 65 °C for 15 min. Homogenization was performed at 70 °C and at pressures of 175 kg/cm^2 for the first stage and 30 kg/cm^2 for the second stage. This was followed by pasteurization at 85 °C for 30 s and chilling at 4 °C, both in a tubular exchanger. The mix was matured in an agitated tank (60 rpm) at 4 °C for 16 h.

Freezing. Freezing was performed in a scraped surface heat exchanger (Technohoy MF 50), with about 100% overrun. The temperature of the mix was lowered to −5 °C. The ice cream was packed in 100 mL pots for further analysis, hardened for 1 h at −35 °C, and stored at −25 °C.

Cold Transport and Storage. A specimen (500 mL) of the mix was transported to Cemagref (Rennes, France) on the early morning of day 2 for NMR analysis. A special preliminary study had shown that the NMR signal was not sensitive to the aging of the mix at 4 °C over a period of 24 h. The mixes were transported in an insulated container, and their temperature was checked on reception (4 ± 3 °C). The samples were then placed in a cold chamber at 4 °C for sampling. The ice cream (100 mL) was transported in a single batch once the experimental design was completed. It was transported in dry ice (−78 °C). On reception, the ice cream was stored in a freezer at −27/−28 °C until the day of measurement. The NMR measurements were performed on day 31 (±3 days).

NMR Measurements. Before the NMR measurement, the tube was placed in the NMR probe for thermal equilibration. The probe temperature was controlled using a cryostat (Ministat Huber, Bioblock Scientific). The measurement temperatures were 4 °C (±0.3 °C) for

the mix and −14 °C (±0.3 °C) for the ice cream. The time needed to reach thermal equilibrium at the different measurement temperatures had previously been determined using a series of reference samples fitted with a thermocouple (type T, Ø1 mm). Once the temperature had been stabilized within the sample, NMR measurements were performed with a Bruker spectrometer (Minispec Bruker PC 120, 20 MHz, 0.47 T). The spin−spin relaxation (T_2) was measured from the free induction decay (FID) and the Carr−Purcell−Meiboom−Gill (CPMG) sequences. The spin−lattice relaxation (T_1) was measured from a saturation recovery sequence.

For each formulation, NMR measurements were made in triplicate (for the ice cream) or more (for the mix, fat, and aqueous phase). Results are expressed as a mean value with its standard error.

Sampling for NMR Measurements. The specimen of mix was agitated before a sample was taken with a pipet in a cold chamber at 4 °C. For each new measurement at −14 °C (ice cream), the sample (approximately 0.3 g) was placed in an enclosed space (glovebox) thermostatically controlled at −18 °C. The top layer of the sample (the part of the product most sensitive to temperature fluctuations) was removed, and the sample used to fill the NMR tubes was taken from the core of the sample using a punch. The NMR tubes (Ø10 mm) were filled to a height of 10 mm for all measurements.

Processing of the NMR Relaxation Signals and Expression of the Results. Different components, numbered 1, 2, etc., may be encountered if protons belong to different molecules (e.g., sugar protons and water protons) or if they are involved in different physical states (liquid or solid).

For the spin−spin relaxation, the relaxation decay curves were fitted to a series of Gaussian (FID) and exponential (CPMG) decays using the equation:

$$I(t) = \sum_{k'=1}^{n} I(k')e^{-[t/T_{2(k)}]^2} + \sum_{k=1}^{n} I(k)e^{-t/T_{2(k)}} + \text{cst} \qquad (1)$$

where $I(t)$ is the intensity of the relaxation signal, t is the time of the relaxation process, T_2 is the spin−spin relaxation time of component k, and I is the associated intensity. k' and k refer to any of the relaxing components in the FID (solid phase) and the CPMG (liquid phase), respectively; k and k' will be given in parentheses following T_2, T_1, and I. Equation 1 is valid only for the relaxation decay curve of the samples of mix and ice cream. For anhydrous fat, eq 2 was used to take into account the effect of crystal cell orientation relative to the magnetic field B_0, which induced a Pake pattern

$$I(t) = I(k')e^{-[t/T_{2(k')}]^2} \times \frac{\sin(at)}{at} + [1 - I(k')]e^{-[t/T_{2(k')}]^2} + \sum_{k=1}^{n} I(k)e^{-t/T_{2(k)}} + \text{cst} \qquad (2)$$

The sin $(at)/at$ is an empirical function with an adjusting parameter, a, to take the Pake pattern of the solid phase relaxation into account.

For the spin−lattice relaxation, the relaxation signal from the solid and the liquid phases was adjusted separately using a multiexponential model:

$$I(t) = \sum_{k=1}^{n} I(k)[1 - \alpha e^{-t/T_{2(k)}}] \qquad (3)$$

where $T_1(k)$ is the spin−lattice relaxation time of component k and α is a parameter that takes the imprecision of the pulse angle into account (it equals unity for an ideal 90° pulse).

Relaxation time values and the corresponding intensities are known to be sensitive to the fitting method. To avoid any misadjustment, the relaxation decay curves were first adjusted by the maximum entropy method (MEM) (*23*) as it does not require any initialization of the parameters or choice of a number of exponential functions. With this method, $I(k)$ in eqs 1 and 3, respectively, were replaced by a distribution function of I and the results were presented as a relaxation time distribution. As a second step, the relaxation curves were adjusted by a discrete method (Levemberg−Marquardt algorithm) (*24*), with the number of relaxation components estimated from the MEM. If the relaxation time value and the corresponding amplitude obtained from both methods were in agreement, only the T_1, T_2, and I values from the discrete method are presented, because of their better accuracy.

Table 3. Spin–Spin and Spin–Lattice Relaxation Times with Their Amplitudes for the Aqueous Phase at 4 °C (Only the Results of the Discrete Method of Adjustment Are Presented)

	aqueous phase[a]	water/sucrose solution[b]
	spin–spin relaxation	
T_2 (1) (ms)	**12** (± 4)	**58** (± 7)
T_2 (2) (ms)	**137** (± 2)	**489** (± 6)
I (2) (%)	89.4 (± 1.0)	93.0 (± 0.7)
	spin–lattice relaxation	
T_1 (1) (ms)	**85** (± 4)	**94** (± 0.5)
T_1 (2) (ms)	**514** (± 6)	**636** (± 5)
I (2) (%)	89.4 (± 0.7)	87.0 (± 0.5)

[a] The aqueous phase includes all mix ingredients except fat; in particular, hydrocolloids have been incorporated. [b] From ref *10*, 42.86 g of sucrose per 100 g of water.

The different concepts used for the attribution of the different components are introduced below. The total intensity of the NMR signal, M_0 (in volts), can be expressed as a mass intensity (in volts per gram):

$$MI_i = \frac{I_0}{m_i} \qquad (4)$$

where m is the mass of sample i (g). Knowing the mass fraction of one ingredient (e.g., water), its contribution to the signal intensity of the mix can be deduced from the mass intensity. Similarly, knowing the mass intensities of the different components (aqueous phase, fat) together with their fractions in the mixture (**Table 2**), the expected intensity of a given mix can be estimated from the equation:

$$MI_M = \omega_{\text{fat}} MI_{\text{fat}} + \omega_{\text{aqphase}} MI_{\text{aqphase}} \qquad (5)$$

where ω_{fat} and $\omega_{\text{aq phase}}$ are the mass fractions of the anhydrous fat and the aqueous phase (g/g of product), respectively.

The mass intensity of component i can be calculated from the mass intensity of component i at the same temperature, using the equation:

$$MI_j = \frac{MI_i \, \text{PD}_i}{\text{PD}_j} \qquad (6)$$

where PD is the proton density (ratio of the molar mass of the protons to the molar mass of the molecule). For instance, the proton densities of the water, sucrose, lactose, and proteins can be deduced from their chemical formulas and are 0.1111, 0.0643, 0.0643, and approximately 0.06, respectively.

RESULTS AND DISCUSSION

Analysis of the NMR Signal from the Aqueous Phases. Optimum adjustment of the T_2 or T_1 relaxation signal was achieved by a biexponential function (**Table 3**). The result was independent of whether the adjustment method was discrete or continuous (MEM). As the aqueous phase is primarily composed of water and sugar, the attribution of the two relaxation components can be discussed on the basis of already published results describing the relaxation of sucrose solutions. For instance, described is the T_1 and T_2 relaxation of a 42.86% sucrose solution (g sucrose/100 g water) at 4 °C by a biexponential (**Table 3**), the first component of which was attributed to the relaxation of the nonexchangeable protons of the sucrose and the second to the relaxation of water protons,

Table 4. Spin–Spin and Spin–Lattice Relaxation Times with Their Intensities for Anhydrous Fats at 4 °C

Spin–Spin Relaxation		
	fat 1	fat 2
	solid	
T_2 (1) (ms)	**0.033** (± 0.002)	**0.045** (± 0.002)
I (1) (%)	38.6 (± 2.8)	49.0 (± 2.7)
a	133 (± 2)	152 (± 2)
T_2 (2) (ms)	**0.044** (± 0.003)	**0.027** (± 0.001)
I (2) (%)	10.1 (± 0.6)	32.0 (± 2.7)
	liquid	
T_2 (3) (ms)	**7.4** (± 0.2)	**14.2** (± 1.2)
I (3) (%)	26.3 (± 1.1)	**9.5** (± 1.2)
T_2 (4) (ms)	**29.5** (± 0.8)	**56.9** (± 1.2)
I (4) (%)	24.9 (± 1.6)	9.5 (± 0.5)
Spin–Lattice Relaxation		
	fat 1	fat 2
	solid	
T_1 (1) (ms)	**349** (± 13)	**818** (± 20)
I (1) (%)	48.0 (± 1.7)	75.0 (± 0.2)
	liquid	
T_1 (2) (ms)	**55** (± 1)	**60** (± 3)
I (2) (%)	39.2 (± 1.2)	20.5 (± 1.3)
T_1 (3) (ms)	**198** (± 15)	**252** (± 54)
I (3) (%)	12.7 (± 1.7)	4.7 (± 1.1)

the exchangeable protons and some of the nonexchangeable protons of the sucrose (*10*). We note that the T_1 relaxation time values and the relative intensity of the signal from the protons of the aqueous phase were consistent with the measured values of a sucrose solution with an equivalent water content. The discrepancy observed in the T_2 relaxation times between the aqueous solution of the mix and the sucrose solution was explained by the protein content of the aqueous phase of the mix. At this concentration (3.23 g/100 g water), the milk proteins induce a strong reduction in the spin−spin relaxation of the water protons (*25*, *26*), whereas the spin−lattice relaxation is far less sensitive to the specific presence of the proteins. To validate this attribution more precisely, we compared the intensity of the expected signal for the water alone with the intensity of the signal from the second component, $I(2)$, measured experimentally for each sample of mix. The expected signal from the water alone is deduced from the mass of the water of each sample and the mass intensity of the water. The discrepancy over all samples (eight formulations × three triplicates) was 2.6 ± 2%. This indicated that 98% of the intensity of the second component, $I(2)$, was represented by the water protons. The intensity of the first component, $I(1)$, therefore described the relaxation of the protons of the sugars and proteins. The estimated proton density was 0.04, which was consistent with the expected proton density (of the order of 0.06), given that the exchangeable protons are not taken into account in the first calculation.

Analysis of the NMR Signal from the Anhydrous Fats. At 4 °C, the relaxation times and the associated intensities were obtained by adjusting a signal reconstructed from the signal acquired by a single 90° (FID) pulse and from the CPMG signal. This allowed all of the T_2 relaxation components of both the liquid fraction and the crystallized fraction to be obtained.The spin−spin relaxation signal from the crystallized fat fraction was described by a relaxation component adjusted by two Gaussian functions (**Table 4**). This Gaussian behavior is classically observed for protons involved in molecules in the crystallized or amorphous state (*27*). The theoretical model to describe the relaxation of molecules in the crystalline state consists of Pake functions (*28*). The latter depend on several parameters, including the orientation of the crystals relative to the B_o field, the dipolar coupling constant, and an order parameter. Even though the parameters can be estimated for pure triglyceride (*29*), they cannot be obtained for mixtures such as milk fats. In this case, the Gaussian model described by eq 2 is used. Correct adjustment of the spin−lattice relaxation signal was achieved by a monoexponential. The amount of crystals at 4 °C estimated from the sum of the intensities of the two Gaussians, $I(1)$ and $I(2)$, varied greatly according to the origin of the fats (**Table 4**). It was 49 ± 3% for the milk fat and 81 ± 6% for the vegetable fat. The variation in the proportion of solid matter and the differences in the relaxation times of the crystallized fraction for both the spin−spin and the spin−lattice relaxations were primarily explained by the fact that each fat has a different triglyceride composition (*30*−*32*).

To estimate the crystal fraction from the spin−lattice relaxation, the intensity of the signal acquired at 11 μs was corrected by the effect of the decrease in the signal induced by the spin−spin relaxation. In fact, the total intensity is obtained at $t = 0$ μs. Because the signal relaxes between 0 and 11 μs through the effect of the spin−spin relaxation with T_2 time constants of the order of 30 and 40 μs (**Table 4**), the result is a loss of signal. The value of $I(t = 0)$ can be estimated by taking this effect into account. Allowing for measurement uncertainty, perfect consistency is observed between the amounts of crystallized fraction deduced from the spin−spin and the spin−lattice relaxations (**Table 4**).

The relaxation of the liquid fraction of the fat protons was more complex. Both the spin−spin and the spin−lattice relaxations were characterized by a wide distribution of relaxation times (**Figure 1**). Optimum adjustment of the relaxation curves by the discrete method was achieved by a biexponential model (**Table 4**). It is not possible, however, to attribute the intensities and the relaxation times to particular proton fractions (*17*). In fact, the relaxation time of a triglyceride is modulated by both the length of the carbon chain and the number of unsaturations (*31*). In the case of a triglyceride mixture, the relaxation signal reflects the mixture's complexity and discrete adjustments are unsuitable to describe this type of behavior.

Analysis of the NMR Signal from the Mixes. The relaxation signal could be adjusted by the Marquardt algorithm using a Gaussian and biexponential model (**Table 5**) regardless of the formulation and the type of relaxation (spin−spin or spin−lattice). We distinguished between a first "solid" component attributable to a crystallized phase and two other "liquid" components attributable to a fraction of the liquid phase of the mix (**Table 5**). Moreover, the biexponential behavior of the liquid fraction was consistent with the result of the continuous method of adjustment (**Figure 2**). Two peaks can be identified for the spin−spin relaxation. The first peak for sample P2F1E2/1 was centered at 30 ms, and the second was centered at 250 ms. These three components can be attributed to the different proton fractions of the mix on the basis of the data obtained for the aqueous phases and the individually isolated fats. Using the intensity data, we checked that the expected intensity of the NMR signal from the mix was the same as the sum of the expected intensities for the aqueous phase and the anhydrous fat at the same temperature. The intensities were weighted according to their proportions in the mix. The discrepancy over all samples between the measured total intensity of the mix and the expected total intensity calculated from its formulation was

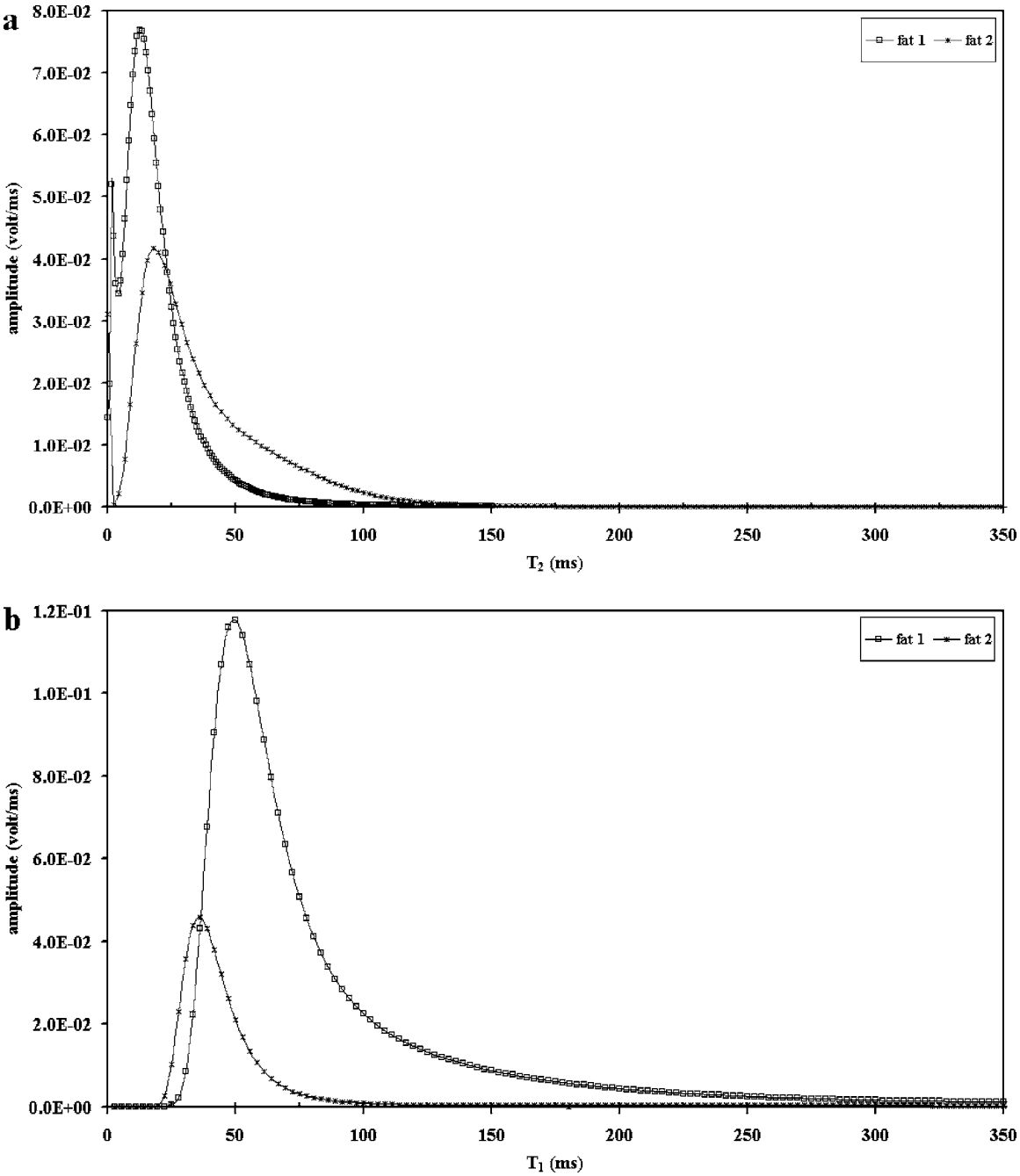

Figure 1. Distribution of (**a**) spin–spin and (**b**) spin–lattice relaxation times obtained by MEM for the liquid fat at 4 °C.

0.5 ± 1.9% (**Table 6**). This shows that the adjustment of the NMR signal from the mix was conservative and was perfectly consistent with the composition of the mix.

The attribution approach is illustrated using the spin−spin relaxation of the mixes (**Tables 5** and **6**). It can be extrapolated to the spin−lattice relaxation. The longest relaxation time [$T_2(3) \approx 145$ ms for formulas P2F1E2/1 and P2F2E1/1 and $T_2(3) \approx 154$ ms for formulas P2F1E1/1 and P2F2E2/1] could be attributed to the relaxation of the water protons and to the exchangeable protons of the sugars. The relaxation time values were consistent with the relaxation of the water protons and the exchangeable protons of the sugars of the aqueous phase: $T_2(2) = 137$ ms (**Tables 3** and **5**). Moreover, the estimated intensity (in volts) for the water in the aqueous phase is the same as the adjusted intensity for this last component. The difference between the two intensities is 7.6 ± 2% for all samples, taking the different masses of each tube into account (**Table 6**). The relaxation of the water protons therefore contributes about 93% of the third component of the mix, $T_2(3)$.

The first (solid) component of the mix, $T_2(1)$, can be attributed to the crystallized fat, the only possible solid component present. The contribution of the nonexchangeable protons of the proteins is in fact too small to be detected at this concentration, and the solid component was absent in the aqueous phase. When the mix samples were heated to 40 °C, all of the fat was liquid and no solid component of the mix was detected (**Figure 3**). The difference in relaxation time and the change of adjustment model (**Tables 4** and **5**) resulted primarily from the low fat content of the emulsions. The signal intensity in the mixes was not high enough for it to be adjusted with two Gaussians. Moreover, it has been shown that the spin−spin relaxation can vary according to the structure of the fat crystals (*29*). Given that the crystalline structure of anhydrous fats and fats in emulsion can be different,

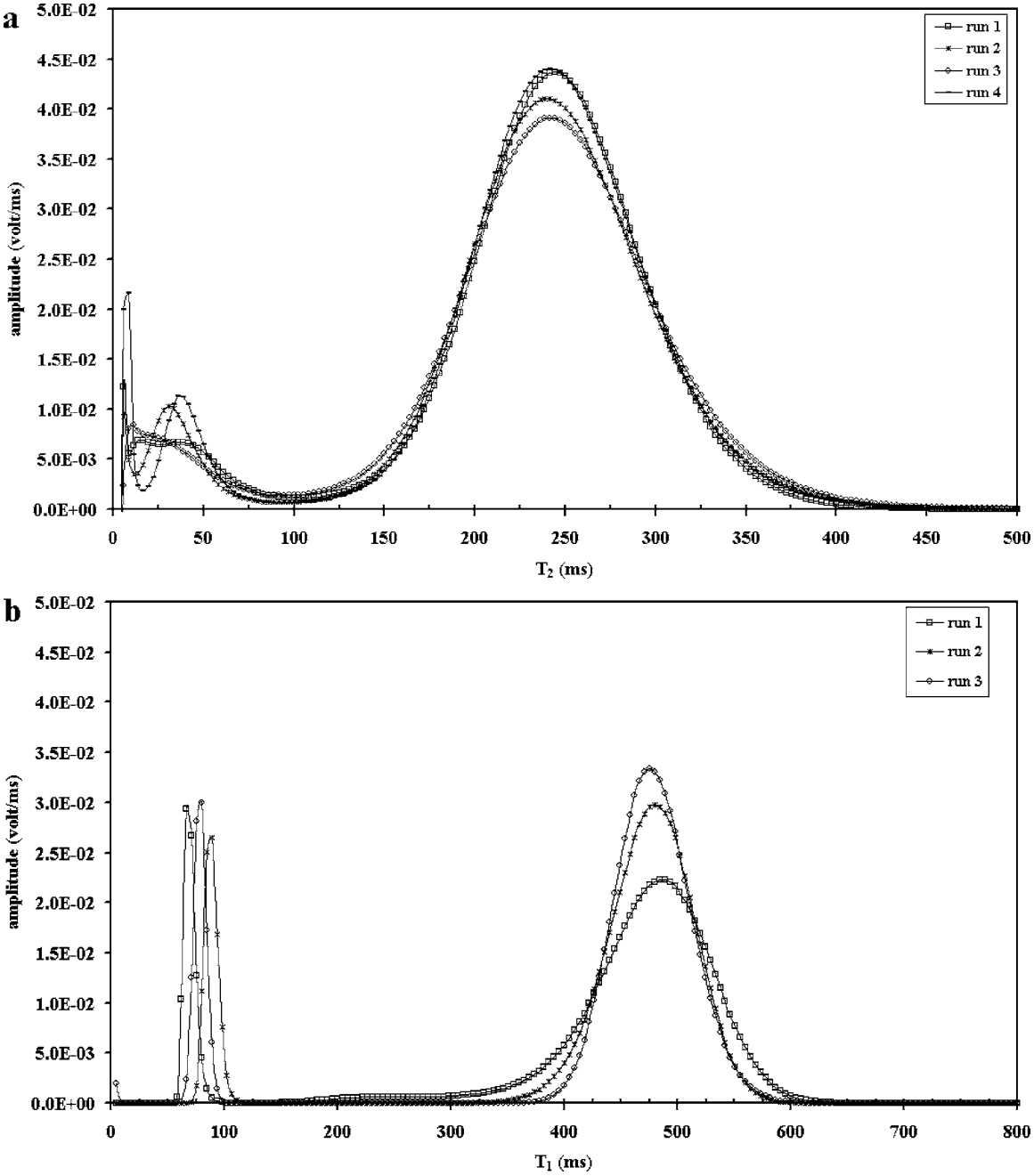

Figure 2. Distribution of (**a**) spin–spin and (**b**) spin–lattice relaxation times obtained by MEM for the liquid phase in mix P2F1E2/1 at +4 °C (three samples).

this probably also contributed to the observed discrepancies in the relaxation time of the first component.

The $T_2(2)$ relaxation time was close to that observed for the (nonexchangeable) sugar protons of the aqueous phase and was centered on the distribution of the T_2 relaxation times of the pure liquid fat. It appeared quite consistent that the relaxation of the sugar protons and that of the protons of the liquid fat were found in the second (liquid) component observed in the mixes. Moreover, quantitative analysis of the intensities led us to demonstrate that the intensity of the total signal from the mix was equivalent to the sum of the intensities of the fat signals and those from the aqueous phase and that the intensity of the third component of the mix was explained by the intensity of the aqueous phase. It also led us to demonstrate that the intensity of the first component was explained by the intensity of the crystallized fat. This validates the attribution of the second component to the relaxation of the nonexchangeable protons of the sugars and to the protons of the liquid fat.

Analysis of the NMR Signal from the Ice Cream. The spin−spin relaxation signal from the ice cream can be broken down into one Gaussian and two exponential functions regardless of the formulation (**Table 5**). We found the same distribution as for the mixes, i.e., a first solid component and two liquid components, whatever the fitting method used. However, discrepancies between the two different methods were observed in the respective intensities of the two liquid exponentials. This is explained by the fact that the two components identified by the MEM are not completely separated (**Figure 4**). The first (solid) component includes the relaxation both of the protons of the crystallized fat and of the ice. In fact, the T_2 relaxation times of the ice protons and the protons of the crystallized fat are too close to be separated. At −14.4 °C, the T_2 relaxation

Table 5. Spin–Spin and Spin–Lattice Relaxation Times with Their Intensities for Mixes at 4 °C and Ice Creams at –14 °C

		Mix			
		P2F1E2/1	P2F2E2/1	P2F1E1/1	P2F2E2/1
		spin–spin relaxation			
solid	T_2 (1) (ms)	**0.025** (± 0.007)	**0.021** (± 0.002)	**0.026** (± 0.003)	**0.022** (± 0.001)
	I (1) (%)	5.7 (± 1.2)	7.1 (± 0.5)	5.1 (± 0.4)	7.3 (± 0.2)
liquid	T_2 (2) (ms)	**19.4** (± 0.8)	**26.1** (± 1.4)	**22.2** (± 0.7)	**37.8** (± 4.2)
	I (2) (%)	9.4 (± 0.2)	7.8 (± 0.2)	9.5 (± 0.2)	10.0 (± 1.5)
	T_2 (3) (ms)	**145.1** (± 0.3)	**144.0** (± 0.5)	**153.4** (± 0.9)	**156.9** (± 2.8)
	I (3) (%)	85.0 (± 1.0)	85.1 (± 0.5)	85.4 (± 0.4)	82.7 (± 1.3)
		spin–lattice relaxation			
solid	T_1 (1) (ms)	**218** (± 16)	**413** (± 36)	**234** (± 20)	**486** (± 17)
	I (1) (%)	5.5 (± 1.0)	7.0 (± 0.3)	5.0 (± 0.2)	7.0 (± 0.2)
liquid	T_1 (2) (ms)	**80** (± 6)	**73** (± 7)	**76** (± 6)	**76** (± 3)
	I (2) (%)	12.6 (± 0.3)	10.8 (± 0.3)	12.0 (± 0.2)	10.2 (± 0.2)
	T_1 (3) (ms)	**476** (± 2)	**483** (± 4)	**489** (± 4)	**498** (± 1)
	I (3) (%)	81.9 (± 0.8)	82.2 (± 0.2)	83.0 (± 0.2)	82.7 (± 0.2)
		Ice Cream			
		P2F1E2/1	P2F2E2/1	P2F1E1/1	P2F2E2/1
		spin–spin relaxation			
solid	T_2 (1) (ms)	**0.019** (± 0.007)	**0.019** (± 0.002)	**0.017** (± 0.003)	**0.019** (± 0.001)
	I (1) (%)	63.4 (± 1.2)	63 (± 0.5)	67 (± 0.4)	63.3 (± 0.2)
liquid	T_2 (2) (ms)	**0.91** (± 0.04)	**1.78** (± 0.40)	**0.88** (± 0.02)	**1.00** (± 0.02)
	I (2) (%)	15.9 (± 0.2)	13.9 (± 0.6)	15.8 (± 0.0)	15.0 (± 0.3)
	T_2 (3) (ms)	**7.0** (± 0.1)	**9.5** (± 0.8)	**6.9** (± 0.1)	**7.3** (± 0.1)
	I (3) (%)	20.9 (± 0.4)	22.4 (± 0.4)	21.7 (± 0.2)	20.5 (± 0.3)
		spin–lattice relaxation			
solid	T_1 (1) (ms)	**119** (± 10)	**135** (± 18)	**97** (± 25)	**183** (± 50)
	I (1) (%)	8.7 (± 0.4)	7.2 (± 0.6)	8.8 (± 0.5)	8.6 (± 0.0)
liquid	T_1 (2) (ms)	**2223** (± 24)	**1937** (± 55)	**2144** (± 69)	**2149** (± 187)
	I (2) (%)	57.6 (± 3.9)	61.1 (± 0.4)	60.5 (± 0.2)	60.9 (± 2.4)
	T_1 (3) (ms)	**37.3** (± 0.5)	**38.5** (± 0.9)	**38.2** (± 0.2)	**36.4** (± 0.2)
	I (3) (%)	33.7 (± 4.3)	31.7 (± 0.3)	30.6 (± 0.4)	30.5 (± 1.4)

Table 6. Comparison between Experimental Intensities for Mixes and Expected Intensities[a]

	experimental signal amplitude (V) from mixes: I (1) + I (2) + I (3)	total signal intensity (V) expected from the aqueous phase	total signal intensity (V) expected from fat (F1)	Δ V	Δ %	I (3) (V)	total signal intensity (V) expected from water protons
P2F1E2/1	**3.45**	2.99	0.33	**0.12**	3.6	**2.88**	2.61
	3.31	2.95	0.33	**0.03**	1.0	**2.82**	2.57
	3.33	2.99	0.33	**0.01**	0.4	**2.86**	2.61
	3.42	3.06	0.34	**0.02**	0.6	**2.93**	2.67
P2F2E1/1	**3.35**	3.16	0.35	**–0.16**	–4.9	**2.85**	2.76
	3.19	2.85	0.32	**0.03**	0.8	**2.73**	2.48
	3.65	3.22	0.36	**0.07**	1.8	**3.09**	2.81
P2F1E1/1	**3.51**	3.17	0.36	**–0.02**	–0.5	**3.00**	2.77
	3.72	3.32	0.37	**0.03**	0.7	**3.16**	2.90
	3.63	3.25	0.36	**0.01**	0.4	**3.12**	2.84
	3.60	3.24	0.36	**0.00**	0.1	**3.07**	2.82
P2F2E2/1	**3.41**	3.01	0.34	**0.06**	1.9	**2.87**	2.63
	3.41	3.00	0.34	**0.08**	2.3	**2.80**	2.61
	3.24	2.95	0.33	**–0.03**	–1.0	**2.71**	2.57
	3.60	3.22	0.36	**0.02**	0.5	**2.92**	2.81
				mean	0.5		
				standard deviation	1.9		

[a] Left: comparison between the total intensity of the NMR signal from the mixes and the intensities expected from the anhydrous milk fat (F1) and the aqueous phase. Center: difference (Δ) between the adjusted intensities for the mixes and the expected intensities. Right: comparison between the intensity of the third component in the mixes [I (3)] and the intensities expected from the water protons (for the method of calculation, see the text).

time of the ice protons is of the order of 13.1 ± 0.2 μs (*10*) while the relaxation time of the protons of the crystallized fat is of the order of 17.7 ± 0.2 μs.

The third component of the mix, T_2(3), was attributed to the relaxation of the water protons (see previous section). However, this attribution is quite likely not to be possible in the case of ice cream, as the temperature variation and the freeze concentration of the aqueous phase can favor superposition of the water relaxation on the fat relaxation. To attribute this component, we compared the effect of temperature on the relaxation times of a ternary solution (of sucrose and of milk protein) and of ice (*10*) with that of ice cream (using the ice creams manufactured

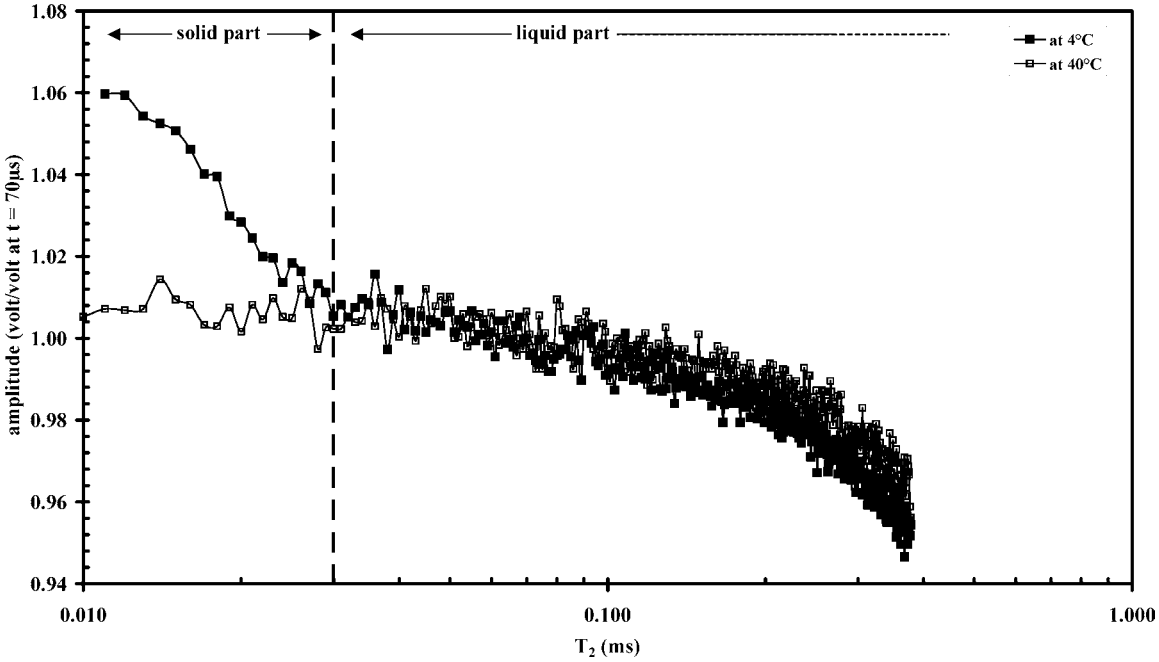

Figure 3. NMR signal from a FID sequence performed on a mix at 4 and 40 °C.

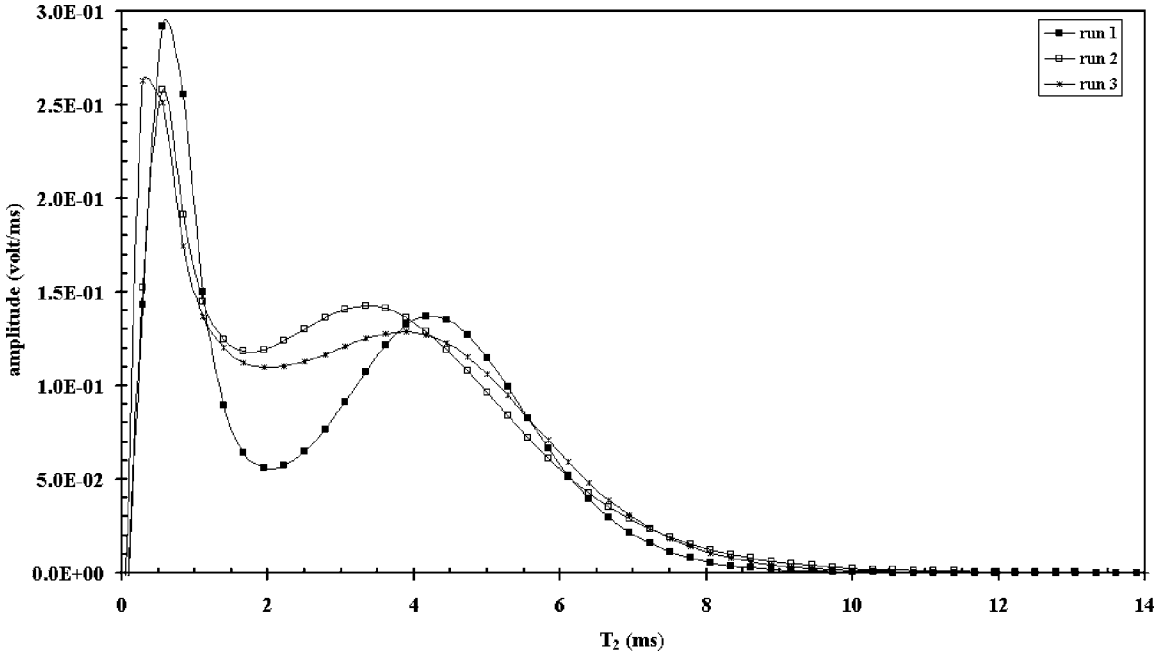

Figure 4. Distribution of spin–spin relaxation times obtained by MEM for the liquid phase in ice cream P2F1E2/1 at –14 °C (three samples).

for this study and a commercial ice cream) (**Figure 5**). Between 0 and −14 °C, the variation in the T_2 relaxation time of the water in the ternary solution containing no fat was identical to that obtained for the $T_2(3)$ relaxation of the commercial ice cream. The variation in the $T_2(3)$ relaxation time of the mix and the ice creams of the experimental design also followed this trend. The discrepancy observed at −14 °C resulted from a difference in the water content relative to the nonfat dry extract in the two matrixes. As the water content of the ice cream was higher, it was normal for the relaxation time to be longer. In other words, the presence of the fat did not modify the behavior of this component, so the third component, $T_2(3)$, can primarily be attributed to the relaxation of the water protons by analogy with the ternary solution.

We applied the same approach to the second component of the liquid fraction, $T_2(2)$ (**Figure 5**), integrating the relaxation behavior of the anhydrous milk fat. We were able to show that the relaxation time of the exchangeable protons of the sugar of the ternary solution and that of the anhydrous milk fat varied according to temperature in complete agreement with the $T_2(2)$ relaxation of the ice cream (**Figure 5**). We therefore conclude that this component described the relaxation of the protons of the liquid fat and the nonexchangeable protons of the sugars.

The spin−lattice relaxation signal of the ice cream has a different behavior from that of the mixes (**Table 5**). The relaxation of the solid phase was described by a biexponential and the relaxation of the liquid phase decreased monoexponentially (instead of behaving biexponentially like the mix). The results were independent of the adjustment method for all formulations. The first solid phase component, $T_1(1)$, very probably corresponded to the relaxation of the crystallized fat. The $T_1(1)$ relaxation time value was consistent with that

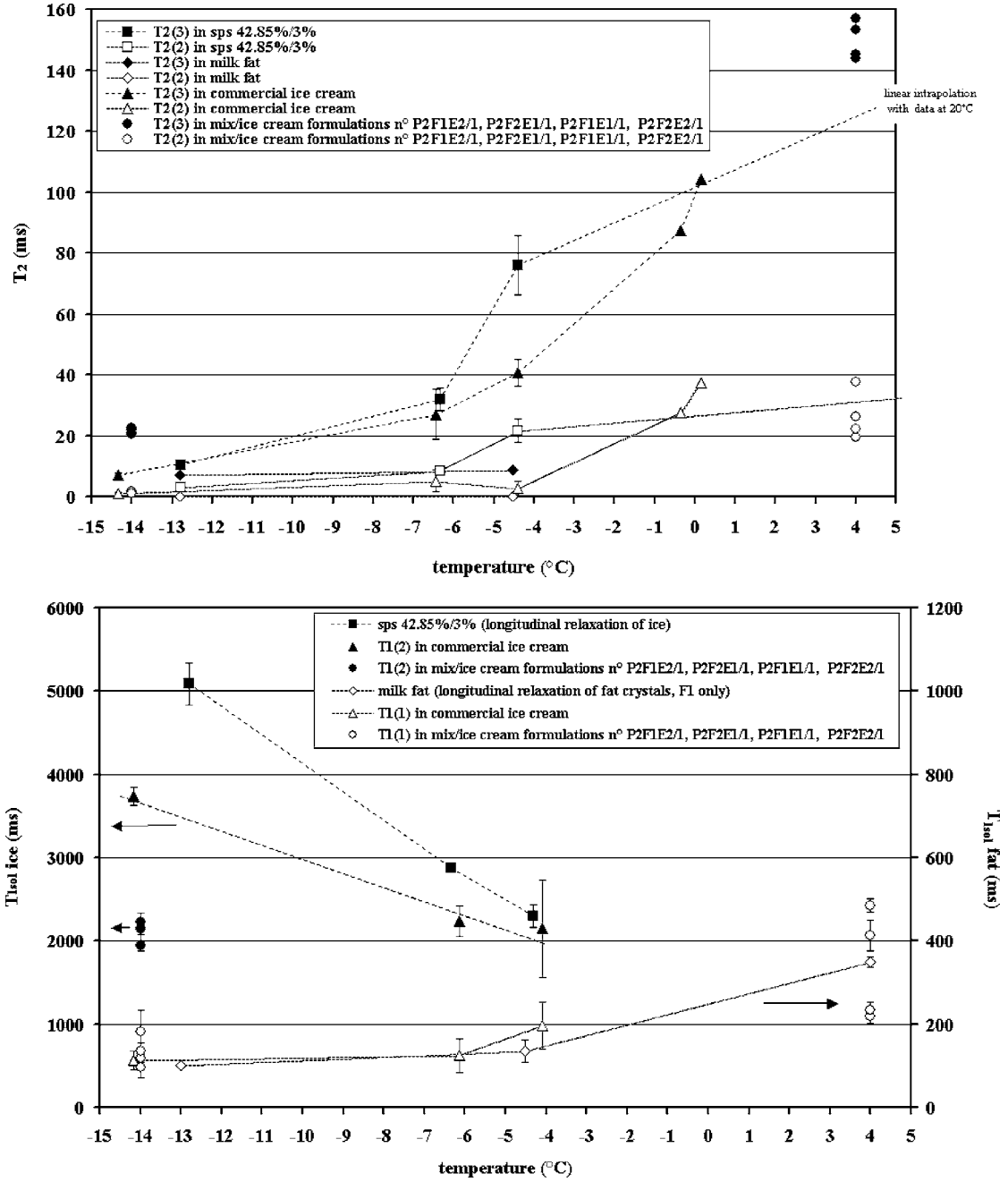

Figure 5. Relaxation times as a function of temperature changes in sucrose/protein solutions (42.85 to 3.05% water basis, noted "sps"), anhydrous milk fat, and commercial ice cream: spin–spin relaxation times for the liquid phase and spin–lattice relaxation times for the solid phases. The relaxation times obtained for mixes P2F1E2/1, P2F2E1/1, P2F1E1/1, and P2F2E2/1 at 4 and −14 °C are superimposed for comparison. Spin–lattice relaxation times: Solid symbols refer to the left-hand axis, and hollow symbols refer to the right-hand axis.

measured for the anhydrous fat (**Figure 5**). The discrepancy was primarily explained by the difference in temperature: 4 °C for the mix and −14 °C for the ice cream. The second solid phase component, $T_1(2)$, was attributed to the relaxation of the ice. Identical relaxation time values have already been observed for fat-free frozen products such as milk protein matrixes (*33*) and dough pieces (*34*). **Figure 5** shows that the evolution of this relaxation component measured in a commercial ice cream was consistent with that observed for a ternary solution of sucrose, milk protein, and water. However, significant discrepancies were observed between the relaxation of the ice of the aqueous solution and that of the ice cream. These will be discussed in another paper (*22*).

The third (liquid phase) component, $T_1(3)$, was attributed to the relaxation of the entire liquid phase. At a temperature of −14 °C, the spin−lattice relaxation can no longer be used to differentiate the behavior of the liquid water from that of the liquid fats or the sugars. The relaxation times were too close, and a mean behavior was observed (**Table 5**).

In conclusion, the ultimate objective of this work was to identify relevant parameters so that the different phases present, the liquid water phase, the crystallized water phase, the liquid fat phase, and the crystallized fat phase, could be monitored, if possible separately, throughout the entire ice cream manufacturing process. The selected parameters and the reasons for their choice are detailed below.

Characterization of the Crystallized Phase of the Water. With the $T_1(2)$ spin−lattice relaxation time, the spin−spin relaxation times of crystals of different molecular natures, such as ice crystals and fat crystals, are too close and this makes it very

difficult to differentiate between them. The spin−spin relaxation component can then not be used to monitor the crystallized water.

Characterization of the Liquid Phase of the Water. The spin−spin and spin−lattice relaxation times $T_2(3)$ and $T_1(3)$ were redundant for monitoring the liquid water in the mix. On the other hand, $T_1(3)$ in the mix has no equivalent in the ice cream: The two components attributed to the liquid phase of the mix, $T_1(2)$ and $T_1(3)$, fuse together to give a single component representative of the liquid phase (liquid water, sugars in solution, liquid fat). This means that the liquid water can be monitored via the spin−spin relaxation time $T_2(3)$ of the mix and the ice cream. It should be emphasized that this also includes the relaxation of the exchangeable protons of the sugars. What is important is to have an NMR parameter that can be used to monitor water relaxation over the whole range of temperatures encountered in ice cream manufacture. The third component of spin−spin relaxation, $T_2(3)$, provides us with qualitative information (interaction between the unfrozen water and the macromolecules) via its relaxation time and to quantitative information via its intensity, $I(3)$.

Characterization of the Crystallized Phase of the Fat. With fhe $T_1(1)$ spin−lattice relaxation time in the mix and in the ice cream, the intensity of the $T_2(1)$ spin−spin relaxation time of the crystallized fractions was used to calculate the solid/liquid ratio in the mix. In the ice cream, the calculation was complicated by the multiple nature of the crystalline phase (crystallized fat, crystallized water). It might be possible at a future date to develop a method based on the intensity of the spin−lattice relaxation of the crystallized fat.

Characterization of the Liquid Phase of the Fat. As for the liquid phase of the water, the spin−lattice relaxation cannot be used as only one component is measured for the T_1 relaxation of the protons of the liquid fat, the sugars, and the water in the ice cream. The liquid fat cannot be monitored via the $T_2(2)$ spin−spin relaxation parameter since this component described both the nonexchangeable protons of the sucrose and the liquid fat protons.

In conclusion, the attribution of the relaxation parameters showed that despite the compositional and structural complexity of ice cream, NMR can be used to monitor the behavior of the fat crystals, the ice, and the aqueous phase. Information on the phases present can be measured, both dynamic information based on the relaxation times and quantitative information such as the amount of crystals. The technique can also in the future be used to determine whether the behaviors of the mix and the ice cream originate in the aqueous or in the fat phase and in the liquid or in the crystallized phase, according to the formulation and process variables.

ACKNOWLEDGMENT

We thank Mr. Barey for helpful scientific discussions and Mr. Evans for the English translation.

LITERATURE CITED

(1) Barfod, N. M. Methods for characterization of structure in whippable dairy-based emulsions. In *Characterization of Food Emerging Methods*; Gaonkar, A. G., Ed.; Elsevier: New York, 1995; pp 59−91.

(2) Donhowe, D. P.; Hartel, R. W.; Bradley, R. L. Determination of ice cream crystal size in frozen desserts. *J. Dairy Sci.* **1991**, *74*, 3334−3344.

(3) Bolliger, S.; Wildmoser, H.; Goff, H. D.; Tharp, B. W. Relationships between ice cream mix viscoelasticity and ice crystal growth in ice cream. *Int. Dairy J.* **2000**, *10*, 791−797.

(4) Caldwell, K. B.; Goff, H. D.; Stanley, D. W. A low-temperature scanning electron microscopy study of ice cream. I. Techniques and general microstructure. *Food Struct.* **1992**, *11*, 1−9.

(5) Chen, C. S. Thermodynamic analysis of the freezing and thawing of foods: Enthalpy and apparent specific heat. *J. Food Sci.* **1985**, *50*, 1158−1162.

(6) Cogné, C.; Andrieu, J.; Laurent, P.; Besson, A.; Nocquet, J. Experimental data and modelling of thermal properties of ice creams. *J. Food Eng.* **2003**, *58*, 331−341.

(7) Weisser, H.; Harz, H. P. NMR studies of foods at sub-freezing temperatures. In *Engineering and Food. I. Engineering Sciences in the Food Industry*; McKenna, B., Ed.; Elsevier Applied Science Publishers: London, 1984; pp 445−454.

(8) Li, S.; Dickinson, L. C.; Chinachoti, P. Mobility of "unfreezable" and "freezable" water in waxy corn starch by ^{2}H and ^{1}H NMR. *J. Agric. Food Chem.* **1998**, *46*, 62−71.

(9) Katayama, S.; Fujiwara, S. NMR study of the freezing/thawing mechanism of water in polyacrylamide gel. *J. Phys. Chem.* **1980**, *84*, 2320−2325.

(10) Lucas, T.; Mariette, F.; Dominiawsyk, S.; Le Ray, D. Water, ice and sucrose behaviour in frozen sucrose-protein solutions as studied by 1H NMR. *Food Chem.* **2003**, *84*, 77−89.

(11) Belton, S.; Boetzel, R.; Bord, E. Interactions between protein and solute molecules in aqueous solutions below 273K. *Sci. Aliments* **1997**, *17*, 145−154.

(12) Goff, H. D.; Freslon, B.; Sahagian, M. E.; Hauber, T. D.; Stone, A. P.; Stanley, D. W. Structural development in ice cream−Dynamic rheological measurements. *J. Texture Stud.* **1995**, *26*, 517−536.

(13) Martin, D. R.; Ablett, S.; Darke, A. H.; Sutton, R. L.; Sahagian, M. Diffusion of aqueous sugar solution as affected by locust beam gum studied by NMR. *J. Food Sci.* **1999**, *64*, 46−49.

(14) Contreras Lopez, E.; Champion, D.; Hervet, H.; Blond, G.; LeMeste, M. Rotational and translational mobility of small molecules in sucrose plus polysaccharide solutions. *J. Agric. Food Chem.* **2000**, *48*, 1009−1015.

(15) ISO 8292. *1991 Animal and Vegetable Fats and Oils−Determination of Solid Fat Content−Pulsed Nuclear Magnetic Resonance Method*; ISO: Geneva, Switzerland, 1991.

(16) Balinov, B.; Mariette, F.; Soderman, O. NMR studies of emulsions with particular emphasis on food emulsions. In *Encyclopedic Handbook of Emulsion Technology*; Sjoblom, J., Ed.; Marcel Dekker: New York, 2003.

(17) Chaland, B.; Mariette, F.; Marchal, P.; de Certaines, J. H1 nuclear magnetic resonance relaxometric characterization of fat and water states in soft and hard cheese. *J. Dairy Res.* **2000**, *67*, 609−618.

(18) Davenel, A.; Marchal, P.; Guillement, J. P. Rapid cooking control of cakes by low resolution NMR. In *Magnetic Resonance in Food Science*; Belton, P. S., Delgadillo, I., Gil, A. M., Webb, G. A., Eds.; Royal Society of Chemistry: Cambridge, 1994; pp 146−155.

(19) Kokubo, S.; Sakurai, K.; Iwaki, S.; Tomita, M.; Yoshida, S. Agglomeration of fat globules during the freezing process of ice cream manufacturing. *Milchwissenschaft* **1998**, *53*, 206−209.

(20) Dinkelmeyer, A.; Weisser, H. The Fourth International Conference on Applications of Magnetic Resonance to Food Science, Norwich, United Kingdom; Vol. 1, pp A29−A32.

(21) Lucas, T.; Le Ray, D.; Barey, P.; Mariette, F. NMR assessment of mix and ice cream. II. Effect of formulation on liquid and solid fat. *Int. Dairy J.* **2004**, in press.

(22) Lucas, T.; Wagener, M.; Barey, P.; Mariette, F. NMR assessment of mix and ice cream. I. Effect of formulation on liquid water and ice. *Int. Dairy J.* **2004**, in press.

(23) Mariette, F.; Guillement, J. P.; Tellier, C.; Marchal, P. Continuous relaxation time distribution decomposition by MEM. In *Signal Treatment and Signal Analysis in NMR*; N., R. D., Ed.; Elsevier: Paris, 1996; pp 218−234.

(24) Marquardt, D. W. An algorithm for least squares estimations of nonlinear parameters. *J. Soc. Ind. Appl. Math.* **1963**, *11*, 431.

(25) Le Dean, A.; Mariette, F.; Lucas, T.; Marin, M. Assessment of the state of water in reconstituted milk protein dispersions by nuclear magnetic resonance (NMR) and differential scanning calorimetry (DSC). *Lebensm.-Wiss. Technol.* **2001**, *34*, 299−305.
(26) Mariette, F.; Tellier, C.; Brule, G.; Marchal, P. Multinuclear NMR study of the pH dependent water state in skim milk and caseinate solutions. *J. Dairy Res.* **1993**, *60*, 175−188.
(27) Blanshard, J. M. V.; Derbyshire, W.; MacNaughtan, W.; Ablett, S.; Martin, D.; Izzard, M. J. ^{1}H relaxation of hydrated carbohydrate systems. In *Adances in Magnetic Resonance in Food Science*; Belton, P. S., Hills, B. P., Webb, G. A., Eds.; The Royal Society of Chemistry: Cambridge, 1999; p 293.
(28) Abragam, A. *The Principles of Nuclear Magnetism*; Oxford: London, 1961.
(29) van Duynhoven, J.; Dubourg, I.; Goudappel, G. J.; Roijers, E. Determination of MG and TG phase composition by time-domain NMR. *J. Am. Oil Chem. Soc.* **2002**, *79*, 383−388.
(30) Marangoni, A. G.; Lencki, R. W. Ternary phase behavior of milk fat fractions. *J. Agric. Food Chem.* **1998**, *46*, 3879−3884.
(31) Le Botlan, D. J.; Helie, I. A novel approach to the analysis of fats by low resolution NMR spectroscopy: Application to milk and vegetable fats. *Analusis* **1994**, *22*, 108−113.
(32) Shen, Z.; Birkett, A.; Augustin, M. A.; Dungey, S.; Versteeg, C. Melting behavior of blends of milk fat with hydrogenated coconut and cottonseed oils. *J. Am. Oil Chem. Soc.* **2001**, *78*, 387−394.
(33) Le Dean, A. Caracterisation de l'eau dans les produits laitiers: cas des dispersions et des gels egoutes et congeles. Ph.D. Thesis, Institut National Agronomique Paris-Grignon, 2000.
(34) Grenier, A.; Lucas, T.; Davenel, A.; Cambert, M.; Le Bail, A.; Mariette, F. NMR assessment of relaxation time and ice fraction in frozen dough. *J. Cereal Sci.* **2004**, submitted for publication.

Received for review May 4, 2004. Revised manuscript received September 27, 2004. Accepted November 3, 2004. This work was partly financed by the Degussa Texturant Systems company.

JF049294O